BBA - Molecular and Cell Biology of Lipids 1870 (2025) 159562

Contents lists available at ScienceDirect

BBA - Molecular and Cell Biology of Lipids

journal homepage: www.elsevier.com/locate/bbalip

# Cold-induced phosphatidylethanolamine synthesis in liver and brown adipose tissue of mice

Maria Soledad Hidrobo [a,1], Marcus Höring [b,1], Sarah Brunner [b], Gerhard Liebisch [b], Sabine Schweizer [a], Martin Klingenspor [c], Renate Schreiber [d], Rudolf Zechner [d], Ralph Burkhardt [b], Josef Ecker [a,b,*]

[a] ZIEL Institute for Food & Health, Research Group Lipid Metabolism, Technical University of Munich, Gregor-Mendel-Str. 2, 85354 Freising, Germany
[b] Institute of Clinical Chemistry and Laboratory Medicine, University Hospital Regensburg, Franz-Josef-Strauß-Allee 11, 93053 Regensburg, Germany
[c] Chair of Molecular Nutritional Medicine, TUM School of Life Sciences, Technical University of Munich, Gregor-Mendel-Str. 2, 85354 Freising, Germany
[d] Institute of Molecular Biosciences, University of Graz, Heinrichstraße 31/2, 8010 Graz, Austria

ARTICLE INFO

*Keywords:*
Cold exposure
Lipidomics
Lipolysis
Liver lipidome
Phosphatidylethanolamine
PUFA

ABSTRACT

Increasing energy expenditure in brown adipose (BAT) tissue by cold-induced lipolysis is discussed as a potential strategy to counteract imbalanced lipid homeostasis caused through unhealthy lifestyle and cardiometabolic disease. Yet, it is largely unclear how liberated fatty acids (FA) are metabolized. We investigated the liver and BAT lipidome of mice housed for 1 week at thermoneutrality, 23 °C and 4 °C using quantitative mass spectrometry-based lipidomics. Housing at temperatures below thermoneutrality triggered the generation of phosphatidylethanolamine (PE) in both tissues. Particularly, the concentrations of PE containing poly-unsaturated fatty acids (PUFA) in their acyl chains like PE 18:0_20:4 were increased at cold. Investigation of the plasma's FA profile using gas chromatography coupled to mass spectrometry revealed a negative correlation of PUFA with unsaturated PE in liver and BAT indicating a flux of FA from the circulation into these tissues. Beta-adrenergic stimulation elevated intracellular levels of PE 38:4 and PE 40:6 in beige wildtype adipocytes, but not in adipose triglyceride lipase (ATGL)-deficient cells. These results imply an induction of PE synthesis in liver, BAT and thermogenic adipocytes after activation of the beta-adrenergic signaling cascade.

*Abbreviations*

| | |
|---|---|
| Anti A | Antimycin A |
| ATGL | Adipose triglyceride lipase |
| ATP | Adenosine triphosphate |
| BAT | Brown adipose tissue |
| BSA | Bovine serum albumin |
| CCT | Choline-phosphate cytidyltransferase |
| CE | Cholesteryl ester |
| CETP | Cholesterol ester transfer protein |
| Cer | Ceramide |
| CL | Cardiolipin |
| DB | Double bond |
| DG | Diglyceride |
| FA | Fatty acid |
| FAME | Fatty acid methyl ester |
| FC | Free cholesterol |
| FCCP | Carbonylcyanide-4(trifluoromethoxy)-phenylhydrazone |
| FDR | False discovery rate |
| FFA | Free fatty acid |
| FIA | Flow injection analysis |
| FTMS | Fourier-Transform mass spectrometry |
| GC–MS | Gas chromatography-mass spectrometry |
| GL | Glycerolipid |
| GPL | Glycerophospholipid |
| HR-MS | High resolution mass spectrometry |
| HSL | Hormone sensitive lipase |
| IBMX | 3-isobutyl-1-methylxanthine |
| ISO | Isoproterenol |
| iWAT | Inguinal white adipose tissue |

* Corresponding author at: Institute of Clinical Chemistry and Laboratory Medicine, Functional Lipidomics and Metabolism Research, University Hospital Regensburg, Franz-Josef-Strauß-Allee 11, 93053 Regensburg, Germany.
*E-mail address:* josef.ecker@ukr.de (J. Ecker).
[1] Contributed equally.

https://doi.org/10.1016/j.bbalip.2024.159562
Received 5 April 2024; Received in revised form 23 August 2024; Accepted 27 August 2024
Available online 28 August 2024

| | |
|---|---|
| KO | Knockout |
| LPC | Lysophosphatidylcholine |
| LPE | Lysophosphatidylethanolamine |
| LXR | Liver X receptor |
| MSX | Multiplexed acquisition |
| MS/MS | Tandem mass spectrometry |
| MUFA | Monounsaturated fatty acids |
| NL | Neutral lipid |
| OCR | Oxygen consumption rate |
| Oligo | Oligomycin |
| PC | Phosphatidylcholine |
| PC O | Phosphatidylcholine-ether |
| Pcyt2 | CTP: phosphoethanolamine cytidylyltransferase |
| PE | Phosphatidylethanolamine |
| PE O | Phosphatidylethanolamine-ether |
| PE P | Phosphatidylethanolamine-based plasmalogens |
| PG | phosphatidylglycerol |
| PI | Phosphatidylinositol |
| PS | Phosphatidylserine |
| PPARa | Peroxisome proliferator-activated receptor alpha |
| PUFA | Polyunsaturated fatty acid |
| SAFA | Saturated fatty acid |
| SL | Sphingolipid |
| SM | Sphingomyelin |
| SVF | Stromal vascular fraction |
| TG | Triglyceride |
| UCP1 | Uncoupling protein 1 |
| VLDL | Very low-density lipoprotein |
| WAT | White adipose tissue |
| WT | Wildtype |

## 1. Introduction

Increasing energy expenditure through cold treatment is considered as potential strategy to treat obesity and cardiometabolic disease, the main cause of death worldwide [1–3]. Cold stimulates the release of noradrenaline from the sympathetic nervous system, which activates beta-adrenergic receptors. As consequence, free fatty acids (FFA) are released from triglycerides (TG) stored in lipid droplets by adipose triglyceride lipase (ATGL) and hormone-sensitive lipase (HSL) in white (WAT) and in brown adipose tissue (BAT) [4–6]. In BAT mitochondria, FFA fuel β-oxidation and activate uncoupling protein 1 (UCP1) generating heat by non-shivering thermogenesis [7,8]. UCP1 uncouples the electron transport from ATP synthesis, facilitating the transfer of protons from the intermembrane space into the matrix, which increases energy expenditure [9,10]. Although the mechanism of action of UCP1 is still a matter of debate, it is clear that in particular longer-chain unsaturated FFA promote UCP1 function [11–13]. In adult humans, physiologically relevant amounts of BAT and brown adipocytes are detected after cold acclimatization that can be activated by beta-3-adrenergic receptor agonists [14–17]. However, the amount of BAT in humans is negligible compared to the total volume of adipose tissue in the body [18,19]. In contrast, mice, particularly those of the Sv129 strain, contain substantially higher fractions of brown adipocytes than humans (up to 50% of total adipocytes) [20].

Whatever the proportion of BAT, in mice and humans, the amount of FFA liberated after cold-induced lipolysis exceeds the amount necessary for activating UCP1 function. This suggests that excess FFA are metabolized in other tissues, particularly in the liver as central lipid metabolic organ. So far, lipid metabolism after acute and short-term cold exposure was the main focus of research. For example, a recent human trial with 10 volunteers exposed to cold just below the shivering threshold for 0.5 to 2 h indicated that lipolysis-derived FFA are transported to the liver for metabolism to TG, before re-secretion via very low-density lipoproteins (VLDL) into the circulation [21]. In mice, an increased hepatic production and metabolism of acylcarnitines was observed, when animals were exposed to 4 °C for 5 h [22,23]. The knowledge on lipid metabolic pathways altered by prolonged exposure to cold (> 5 days) is limited, especially on those affected in the liver.

In this study, we present a comprehensive picture of systematic lipidomic changes in the liver and BAT induced after long-term cold exposure. Therefore, the liver and BAT lipidome of mice housed at 4 °C, 23 °C and 30 °C for 7 days was investigated using quantitative tandem (MS/MS) and high-resolution mass spectrometry (HRMS). Our analyses revealed that housing below thermoneutrality triggers the generation of polyunsaturated fatty acids (PUFA; ≥ 2 double bonds)-containing phosphatidyl-ethanolamine (PE) in liver and BAT, which depends on FA uptake from the circulation. Using primary beige adipocytes differentiated from preadipocytes isolated from inguinal white adipose tissue (iWAT) of wildtype and ATGL KO mice, we provide further evidence for our findings. Isoproterenol, a beta-adrenergic agonist, elevated intracellular levels of unsaturated PE, i.e. PE 38:4 and PE 40:6, in beige wildtype adipocytes, but not in ATGL-deficient adipocytes.

## 2. Materials and methods

### 2.1. Ethics statement

Mouse experiments were performed in accordance with relevant ethical guidelines. All animal husbandry and experiments for this study were approved by the responsible local authorities (Regierung von Oberbayern; approval numbers: 55.2–1-54-2531-99-13-2015, 55.2–1-54-2532-17-2015, and 55.2–1-54-2532-34-2016).

### 2.2. Mouse housing and experiments

Male 129Sv/ev Tac mice were housed in a specific pathogen-free facility with free access to chow (V1534, Ssniff) and water at 23 °C, 55 % relative humidity and a 12-h light/dark cycle. Ten-week-old mice were housed at either 4 °C, 22 °C or 30 °C for seven days. After that, mice were sacrificed by CO2 asphyxiation. For plasma collection, ≈100 μl of blood were drawn by cardiac puncture, transferred into EDTA tubes (Sarstedt) and centrifuged for 10 min at 1500 ×*g* and 4 °C, before the supernatant was transferred into microtubes until further processing. iBAT, iWAT, eWAT, liver and plasma were collected and immediately snap frozen in liquid nitrogen. Samples were stored at −80 °C until further processing.

### 2.3. Isolation of mitochondria from brown adipose tissue

Mitochondria were enriched from BAT using differential centrifugation as recently described [24]. Per mitochondrial sample, BAT from five male and female mice was pooled.

### 2.4. Primary cell isolation and cell culture

The stromal vascular fraction (SVF) was isolated from inguinal fat depots of male and female WT and global ATGL KO mice [25]. Briefly, fat depots were dissected, minced into small pieces and digested with collagenase type D (Roche) in an orbital shaker at 37 °C for 1 h. After digestion, the cell suspensions were filtered through a 70 μm cell strainer and centrifuged at 1000 x*g* for 5 min. The cell pellet was resuspended in 5 ml of red blood cell lysis buffer for 3 min and washed three times with PBS. Pre-adipocytes were seeded onto 10 cm cell culture plates and cultured in culture medium containing DMEM/F-12 + GlutaMAX™ (Thermo Fisher Scientific), 10 % FCS, 100 IU/l penicillin and 0.1 mg/l streptomycin. Cells were grown to 80 % confluency and cryopreserved until further experiments. Frozen pre-adipocytes were rapidly thawed and cultivated with culture medium. One day after reaching confluency, pre-adipocytes were induced with medium containing DMEM/F-12 + GlutaMAX™, 10 % FBS superior (Sigma-Aldrich), penicillin/streptomycin (0.4 %; Sima-Aldrich), insulin (5 μm/ml),

isobutylmethylxanthine (IBMX) (0.5 mM), dexamethasone (1 μM) and rosiglitazone (1 μM) (Sigma-Aldrich). After 48 h, the induction medium was replaced with differentiation medium (DMEM/F-12 + GlutaMAX™, 10 % FBS superior, penicillin/streptomycin (0.4 %), insulin (5 μg/ml)). Differentiation medium was changed every other day for six days until primary beige adipocytes were harvested for measurement of lipid profiles or for microplate-based respirometry assays.

### 2.5. Microplate-based respirometry

Oxygen consumption of primary beige adipocytes was analyzed in a Seahorse XF Pro analyzer (Agilent Technology) as previously described [26,27]. In brief, beige adipocytes were washed and incubated with respiration medium (pH 7.4) (DMEM base (Sigma-Aldrich), glucose (25 mM; Carl Roth), glutaMAX™ (2 mM; Thermo Fisher Scientific), NaCl (31 mM; Carl Roth)) and essentially fatty acid-free bovine serum albumin (BSA) (2 %; Sigma-Aldrich) at 37 °C for 1 h. Basal respiration was measured first, followed by proton leak-linked respiration induced by oligomycin (5 μM; Sigma Aldrich), UCP1-dependent respiration after isoproterenol (0.5 μM; Sigma-Aldrich), maximal respiratory capacity after carbonyl cyanide-*p*-trifluoromethoxyphenylhydrazone (FCCP) (7 μM; Sigma-Aldrich) and non-mitochondrial oxygen consumption after antimycin A (5 μM; Sigma-Aldrich).

### 2.6. Lipidomics

Lipid species were annotated according to the proposal for shorthand notation of lipid structures that are derived from mass spectrometry [28]. For quantitative lipidomics, non-naturally occurring internal standards were added prior to lipid extraction. A wet weight of 2 mg tissue (liver or adipose tissue), or an amount of 100 μg protein (cell samples) was subjected to lipid extraction according to the protocol by Bligh and Dyer [29]. For analysis of phospholipids in adipose tissue, the dried lipid extract was additionally washed three times with 2,2,4-trimethylpentane (against water) to remove excess neutral lipids. The washed extract was then subjected to a second Bligh and Dyer extraction before mass spectrometric analysis.

The analysis of lipids was performed by direct flow injection analysis (FIA) using a triple quadrupole mass spectrometer (MS/MS) and a high-resolution hybrid quadrupole-Orbitrap mass spectrometer/ Fourier-Transform mass spectrometry (FTMS). FIA-MS/MS was performed in positive ion mode using the analytical setup and strategy described previously [30,31]. A fragment ion of *m/z* 184 was used for lysophosphatidylcholines (LPC) [32]. The following neutral losses were applied: Phosphatidylethanolamine (PE) and lysophosphatidylethanolamine (LPE) 141, phosphatidylserine (PS) 185, phosphatidylglycerol (PG) 189 and phosphatidylinositol (PI) 277 [33]. Sphingosine based ceramides (Cer) and hexosylceramides (Hex-Cer) were analyzed using a fragment ion of *m/z* 264 [34]. PE-based plasmalogens (PE P) were analyzed according to the principles described by Zemski-Berry [35]. Cardiolipin (CL) was quantified using diacylglycerol-specific fragment ions as described previously [36]. Glycerophospholipid species annotation was based on the assumption of even numbered carbon chains only.

A detailed description of the FIA-FTMS method was published recently [37,38]. Triglycerides (TG), diglycerides (DG) and cholesterol esters (CE) were recorded in positive ion mode *m/z* 500–1000 as $[M + NH_4]^+$ at a target resolution of 140,000 (at *m/z* 200). CE species were corrected for their species-specific response [39]. Phosphatidylcholines (PC), PC ether (PC O) and sphingomyelins (SM) were analyzed in negative ion mode *m/z* 520–960 as $[M + HCOO]^-$ at the same resolution setting. Analysis of free cholesterol (FC) was performed (after derivatization with acetyl chloride [31]) by multiplexed acquisition (MSX) of the $[M + NH_4]^+$ of FC and the deuterated internal standard (FC[D7]) [39].

CL in isolated BAT mitochondria was analyzed by FIA-FTMS in negative ion mode in *m/z*-range 1100–1600 as $[M-H]^-$ dissolved in methanol/chloroform = 5/1 (*v*/v) containing 0.005 % dimethylamine. The method quantifies CL species on the sum composition level.

The product ion spectrum of PE 38:4 $[M-H]^-$ was recorded in negative ion mode at a resolution of 35,000 using an isolation window of 1 Da, and a normalized collision energy of 30 %.

A list of all used non-naturally occurring standards for FIA-MS/MS and FIA-FTMS analyses can be found in **Suppl. Data 1**.

Total fatty acid analysis was performed by gas chromatography coupled to mass spectrometry (GC–MS) of fatty acid methyl esters (FAMEs) as described before [40]. Total FA are all occurring fatty acids in plasma, including those bound to complex lipids, such as TG, which were hydrolyzed prior to FAME analysis.

### 2.7. Statistical analysis of lipidomic data

Lipidomic data were analyzed according to the principles described previously [41,42]. For generation of volcano plots, all data were $\log_2$ transformed to ensure that they were normally distributed. Lipid species were excluded if they were undetectable in >50 % of the samples. A standard two-sided, unpaired *t*-test assuming unequal variances was used to test for significantly different abundances in the conditions. The Benjamini–Hochberg method was used to calculate the false discovery rate (FDR) and to account for multiple testing ($p_{adj} < 0.05$). Fold changes were calculated as the difference between mean of the log-transferred values at 4 °C and 23 °C [I]; and 23 °C and 30 °C [II]. To compare mean lipid concentrations between groups a standard two-sided, unpaired *t*-test assuming unequal variances was applied.

## 3. Results

### 3.1. In liver, cold exposure increases polyunsaturated phosphatidylethanolamines

To investigate the lipidomic response to long term cold exposure and lipolysis, 129SvS6 mice were housed at 30 °C (thermoneutrality, $n = 12$), 23 °C ($n = 9$), and 4 °C (n = 9) for 7 days. The liver lipidome was quantified using a comprehensive untargeted lipidomic analysis based on electrospray ionization coupled to MS/MS and HRMS comprising: (1) Glycerophospholipids (GPL): phosphatidylcholine (PC), phosphatidylcholine-ether (PC O), lysophosphatidylcholine (LPC), phosphatidylethanolamine (PE), phosphatidylethanolamine-ether (PE O), lysophosphatidylethanolamine (LPE), phosphatidylglycerol (PG), phosphatidylserine (PS) and phosphatidylinositol (PI). (2) Glycerolipids (GL): diglyceride (DG) and triglyceride (TG). (3) Sterols: free cholesterol (FC) and cholesteryl ester (CE). (4) Sphingolipids (SL): sphingomyelin (SM) and ceramide (Cer). Quantification was based on lipid class-specific internal standards that do not occur naturally.

In total, 241 lipid species were quantified in liver samples (**Suppl. Data 1**). Major lipid classes at 4 °C, 23 °C and thermoneutrality were PC (17.4 nmol/mg, 17.2 nmol/mg, 17.2 nmol/mg), PE (13.1 nmol/mg, 11.5 nmol/mg, 10.2 nmol/mg), PI (10.7 nmol/mg, 9.6 nmol/mg, 9.5 nmol/mg), PS (3.2 nmol/mg, 3.1 nmol/mg, 3.1 nmol/mg), TG (10.7 nmol/mg, 13.9 nmol/mg, 8.8 nmol/mg) and FC (4.6 nmol/mg, 4.6 nmol/mg, 4.8 nmol/mg) (Fig. 1A). SM (0.9 nmol/mg, 0.8 nmol/mg, 0.8 nmol/mg), DG (0.8 nmol/mg, 0.9 nmol/mg, 0.9 nmol/mg), CE (0.5 nmol/mg, 0.7 nmol/mg, 0.6 nmol/mg) and CL (0.7 nmol/mg, 0.7 nmol/mg, 0.7 nmol/mg) were dominating lipid classes of the group of minor lipids (Fig. 1B). To test if the housing temperature affects the hepatic lipidome, lipid concentrations were analyzed in the comparisons **[I]** 4 °C vs. 23 °C and **[II]** 23 °C vs. 30 °C. After correcting for multiple testing by controlling the false discovery rate at 0.05, the levels of 75 (31 % of all) lipid species were found significantly different in comparison **[I]** (Fig. 1C-D), and 124 (51 % of all) lipid species in comparison **[II]** (Fig. 1E-F). Most importantly, 27 lipids were significantly altered and showed the same direction of regulation in both comparisons. Of those, 15 were elevated after housing mice at colder temperatures.

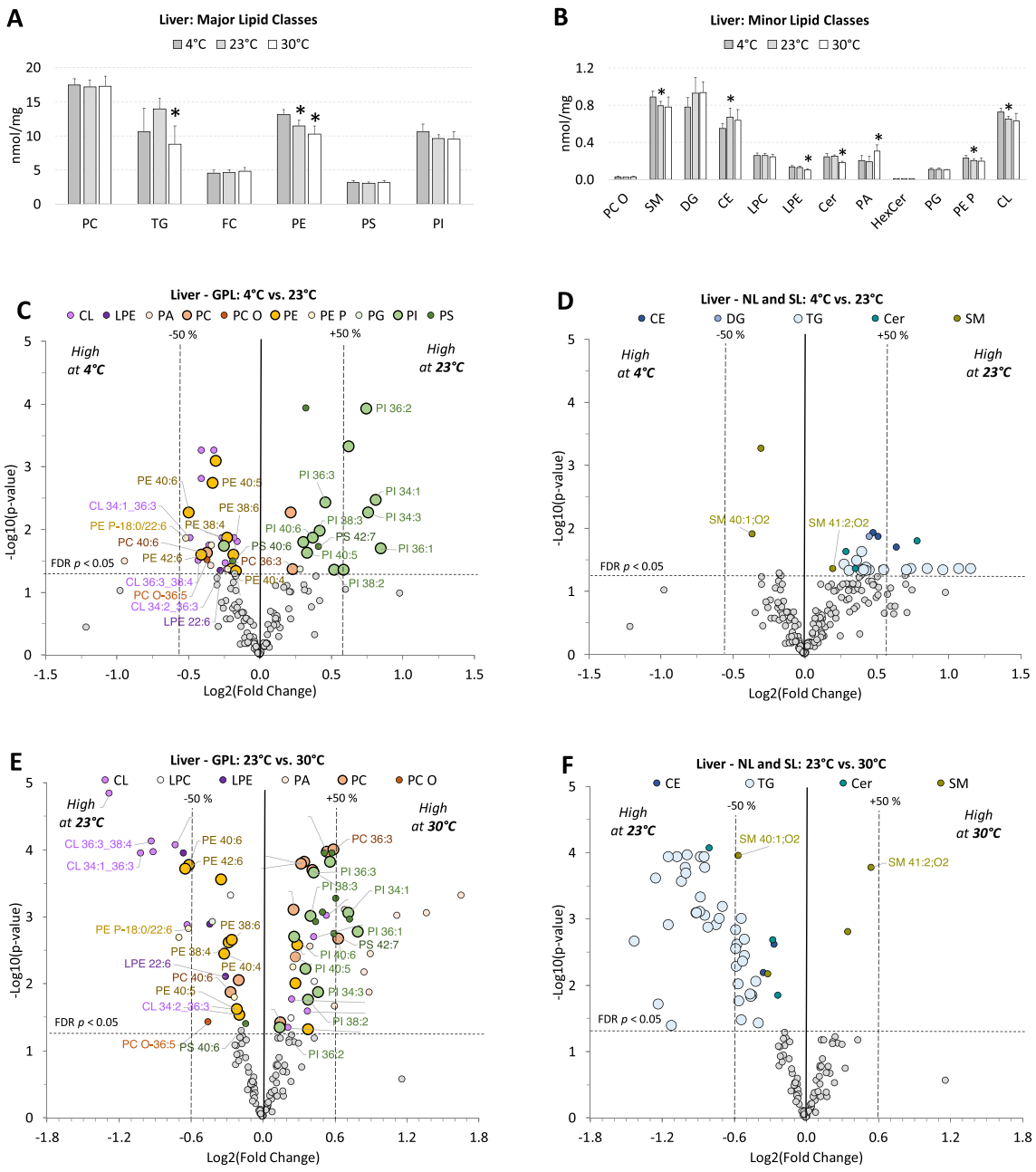


**Fig. 1. Cold exposure increases polyunsaturated PE in liver of mice**

**(A)** Concentrations of major and **(B)** minor lipid classes at cold (4 °C), room temperature (23 °C) and thermoneutrality (30 °C). *$p < 0.05$ indicates a significant difference between groups, determined by a two-sided Student's *t*-test. Shown are means +SD from liver of $n = 9$ (4 °C), n = 9 (23 °C) and $n = 12$ (30 °C). Volcano plots show Log2 fold changes of lipids in liver, whose concentrations are significantly different between 4 °C vs. 23 °C including **(C)** GPL, **(D)** NL and SL; and 23 °C vs. 30 °C including **(E)** GPL, **(F)** NL and SL. Only lipids that were significantly altered and showed the same direction of regulation in both comparisons are labeled in the volcano plots. Large dots indicate lipid species from the major lipid classes. $p < 0.05$ is indicated after correction for multiple testing by controlling for false discovery rate.

These were solely polyunsaturated GPL (except for SM 40:1;O2) including CL 34:1_36:3, CL 34:2_36:3, CL 36:3_38:4, LPE 22:6, PC 40:6, PC O-36:5, PE 38:4, PE 38:6, PE 40:4, PE 40:5, PE 40:6, PE 42:6, PE P-18:0/22:6 and PS 40:6. Cold exposure did not systematically alter total lipid class levels, besides PE, whose concentrations increased with lower housing temperatures (4 °C > 23 °C > 30 °C) (Fig. 1A). Total CL concentrations were similar at 23 °C and 30 °C, but significantly increased only from 23 °C to 4 °C (Fig. 1B). Although in comparison **[I]** and **[II]**, the levels of several PI species were significantly decreased (Fig. 1C, E), total PI levels were similar at all housing temperatures (Fig. 1A).

### *3.2. In BAT, cold exposure elevates polyunsaturated phosphatidylcholine and -ethanolamine*

PE is a major GPL in brown adipocytes [27] and its generation is critical for thermogenesis in BAT of mice [43]. Thus, we analyzed PE as well as other major GPL including PC, PS, PG; the SL: SM, Cer, HexCer; and GL: DG, TG in BAT samples originating from our mice housed at different temperatures.

In BAT, in total, 185 lipids were quantified (**Suppl. Data 1**). The dominating lipid class was TG with 96.5 % (Fig. 2A), for which we could detect 97 individual species. PE (1.3 % and 0.8 %) was the major GPL

analyzed in BAT of mice exposed to 4 °C and 23 °C (Fig. 2B). Comparison of lipid concentrations between different housing temperatures revealed, that levels of 73 (39 % of all) lipid species were found significantly different in comparison **[I]** (Fig. 2C-D), and 121 (65 % of all) lipid species in comparison **[II]** (Fig. 2E-F). Of note, 34 lipids were significantly altered and showed the same direction of regulation in **[I]** and **[II]**, with 11 of them being elevated at colder temperature. Similar to the results found in liver these included, primarily polyunsaturated PE like PE 36:2, PE 36:3, PE 36:4, PE 38:2, 38:4, PE 38:5 and PE 40:4, but also PC 34:2 and PC 36:2; Cer 18:1;O2/22:0 and SM 38:1;O2. Total PE and PC concentrations significantly increased with lower housing temperatures (4 °C > 23 °C > 30 °C) (Fig. 2B). While housing at lower temperature reduced BAT levels of 19 TG species in both comparisons, total TG concentrations significantly dropped from 30 °C to 23 °C, but not from 23 °C to 4 °C (Fig. 2A). Interestingly, the PE species PE 38:4 and 40:4 were increased in both liver (Fig. 1C, E) and BAT (Fig. 2C, E) at colder temperatures in **[I]** and **[II]**.

Because CL detection in BAT was hindered by the adipose tissue matrix, it was quantified in mitochondria isolated from BAT, where CL is highly enriched [44]. Although total mitochondrial CL concentrations were not significantly different in comparison **[I]** and **[II]**, they tended to be higher at 4 °C than at 23 °C and 30 °C (Fig. 2G), which is in agreement with our findings in liver (Fig. 1B). The levels of several CL species containing FA with 68–70 carbons, including CL 68:2, CL 68:3, CL 68:4, CL 70:4 and CL 70:5, were elevated at 4 °C compared to 30 °C, but unchanged between 23 °C and 30 °C (Fig. 2F).

### 3.3. Cold-increased PE 38:4 contains primarily FA 18:0 and FA 20:4 in its acyl chains

Next, we asked what FA are in the acyl chains of cold-induced PE. Therefore, we determined the fatty acyl compositions of PE 38:4 as major PE species (≈ 10 % of total PE) in 3 random liver samples of mice housed at 4 °C applying tandem mass spectrometry. A representative product ion spectrum of PE 38:4 recorded in negative ion mode following collisional induced fragmentation is shown in Fig. 3. We found FA 18:0 (*m/z* 283.2647) and FA 20:4 (*m/z* 303.2329) as most abundant product ions indicating that PE 18:0_20:4 is the major molecular species of PE 38:4. However, we could also detect minor proportions of PE 16:0_22:4 and 18:1_20:3 in the analyzed liver samples. These acyl combinations suggest that FA 16:0, FA 18:0 and FA 18:1 in combination with PUFA (≥ 2 double bonds) containing 20–22 carbons are incorporated into hepatic PE at 4 °C.

### 3.4. Circulating lipids are a potential source for PUFA incorporated in hepatic and BAT PE

Cold-induced generation of PUFA-PE in liver and BAT requires a FA source. Consequently, we asked whether we could find evidence that PUFA incorporated into liver and BAT PE derive from the circulation. Hence, the total FA composition of plasma samples was quantified using GC–MS. We could quantify 30 circulating FA species (**Suppl. Data 1**). Primarily occurring FA were saturated and mono-unsaturated C16–18 FA as well as linoleic acid (FA 18:2 n-6), arachidonic acid (FA 20:4 n-6) and docosahexaenoic acid (FA 22:6 n-3) (Fig. 4A-C). The levels of 19 FA (63 % of all) were significantly increased in comparison **[I]** (Fig. 4D), and 18 FA (60 % of all) in comparison **[II]** (Fig. 4E). The changes of unsaturated (≥ 1 double bond) FA were higher than those of saturated FA (SAFA). For example, in comparison **[I]**, the log2(Fold Changes) of SAFA were in the range of 0.29–0.49, whereas those of mono-unsaturated FA (MUFA) and PUFA were in the ranges of 0.52–0.93 and 0.24–0.89 (Fig. 4D). The concentrations of FA 20:2 n-6, FA 20:3 n-6, FA 20:4 n-3 and FA 22:4 n-6 were significantly lower at colder housing temperatures in comparisons **[I]** and **[II]** (Fig. 4D-E) indicating that circulating lipids represent a potential source for FA, i.e. PUFA, required for hepatic and BAT PE synthesis.

To provide further evidence for this hypothesis, we correlated plasma PUFA with liver or BAT PE species that were significantly increased in comparisons **[I]** and **[II]** (Plasma: FA 20:2 n-6, 20:3 n-6, 20:4 n-3 and 22:4 n-6; Liver: PE 38:4, 38:6, 40:4, 40:5, 40:6, 42:6; BAT: PE 36:2, 36:3, 36:4, 36:5, 38:2, 38:4, 38:5, 38:6). In all tested PE-FA combinations, hepatic PE species were negatively related with plasma FA species with $R^2$ ranging between 0.49 and 0.89 (Fig. 5). The highest correlation coefficients were observed for the correlations of PE 40:6 with FA 20:2 n-6 ($R^2 = 0.87$), FA 20:3 n-6 ($R^2 = 0.89$) and FA 20:4 n-3 ($R^2 = 0.82$). In agreement with the liver data, also BAT PE species negatively correlated with plasma PUFA, with $R^2$ of 0.56–0.90 (**Suppl. Fig. 1)**. Here, the highest correlation coefficients were observed for the combinations PE 36:4 and FA 20:2 n-6 ($R^2 = 0.89$) or FA 20:3 n-6 ($R^2 = 0.90$); and PE 38:4 and FA 20:6 n-3 ($R^2 = 0.89$). These results further support the hypothesis that PUFA metabolized to hepatic and BAT PE can originate from the circulation.

### 3.5. Intracellular lipolysis increases PE 38:4 and 40:6 in beige adipocytes

Finally, we tested whether intracellular lipolysis modulates the production of PUFA-PE. Therefore, PE profiles were analyzed in beige (also called brite) adipocytes differentiated from primary preadipocytes isolated from inguinal white adipose tissue (iWAT) of wildtype (WT) and ATGL KO mice after stimulation with isoproterenol (ISO). ISO is a beta-adrenergic agonist inducing ATGL-mediated lipolysis and in turn, UCP1 [45,46]. Beige adipocytes with a mixed phenotype between white and brown adipocytes [47,48] were chosen, since they contain both, a high ATGL-mediated lipolytic capacity (as observed in white adipocytes) as well as a significant UCP1 activity (typical to brown adipocytes). This was confirmed by analyses of the mitochondrial bioenergetics profile illustrated in Fig. 6A using microplate-based respirometry including: [a] basal respiration; [b] basal uncoupled respiration after blocking ATP synthase with Oligomycin; [c] induction of UCP1 by addition of isoproterenol (ISO) as beta-adrenergic agonist; [d] assessment of the maximal respiratory capacity by using carbonyl cyanide 4-(trifluoromethoxy) phenylhydrazone (FCCP) as uncoupling agent; [e] non-mitochondrial $O_2$ consumption applying antimycin A (Anti A). In WT cells, ISO induced the UCP1-dependent $O_2$ consumption rate ≈2-fold, while in ATGL KO cells no significant UCP1 function could be detected (Fig. 6B-C).

Quantification of PE revealed a significant increase of the PUFA-containing PE 38:4 and PE 40:6 concentrations in WT, but not in ATGL KO cells, after beta-adrenergic stimulation (Fig. 6D). Of note, PE 38:4 was also found increased in liver and BAT samples in the comparisons **[I]** and **[II]** and could be related with circulating PUFA in both tissues. Together, these results provide strong evidence that intracellular lipolysis increases unsaturated PE in thermogenic adipocytes and support our liver and BAT data obtained from the experiments with mice exposed to colder temperatures.

## 4. Discussion

Thermoneutrality is defined as the metabolic state of an organism at an environmental temperature at which it does not need to generate or lose heat [49]. Although most studies highlight the benefits of cold treatment for energy expenditure, it can also have unfavorable effects on physiology and metabolism. Permanent exposure to ambient temperatures below the organism's thermoneutrality can lead to a constant stress level [49,50]. Energy needed for basal cellular functions is redirected towards heat generation to maintain the ideal core temperature, which can affect, for example, the metabolic activity of immune cells and the outcome of diseases including infectious diseases or cancer. Some reports even indicate an induction of ferroptosis, an iron-reliant cell death pathway involving the lethal peroxidation of PUFA in cell membrane lipids by oxygen-containing free radicals [51]. In liver tissue of rats exposed to −10 °C for 8 h, ferroptosis-related markers like $Fe^{2+}$,

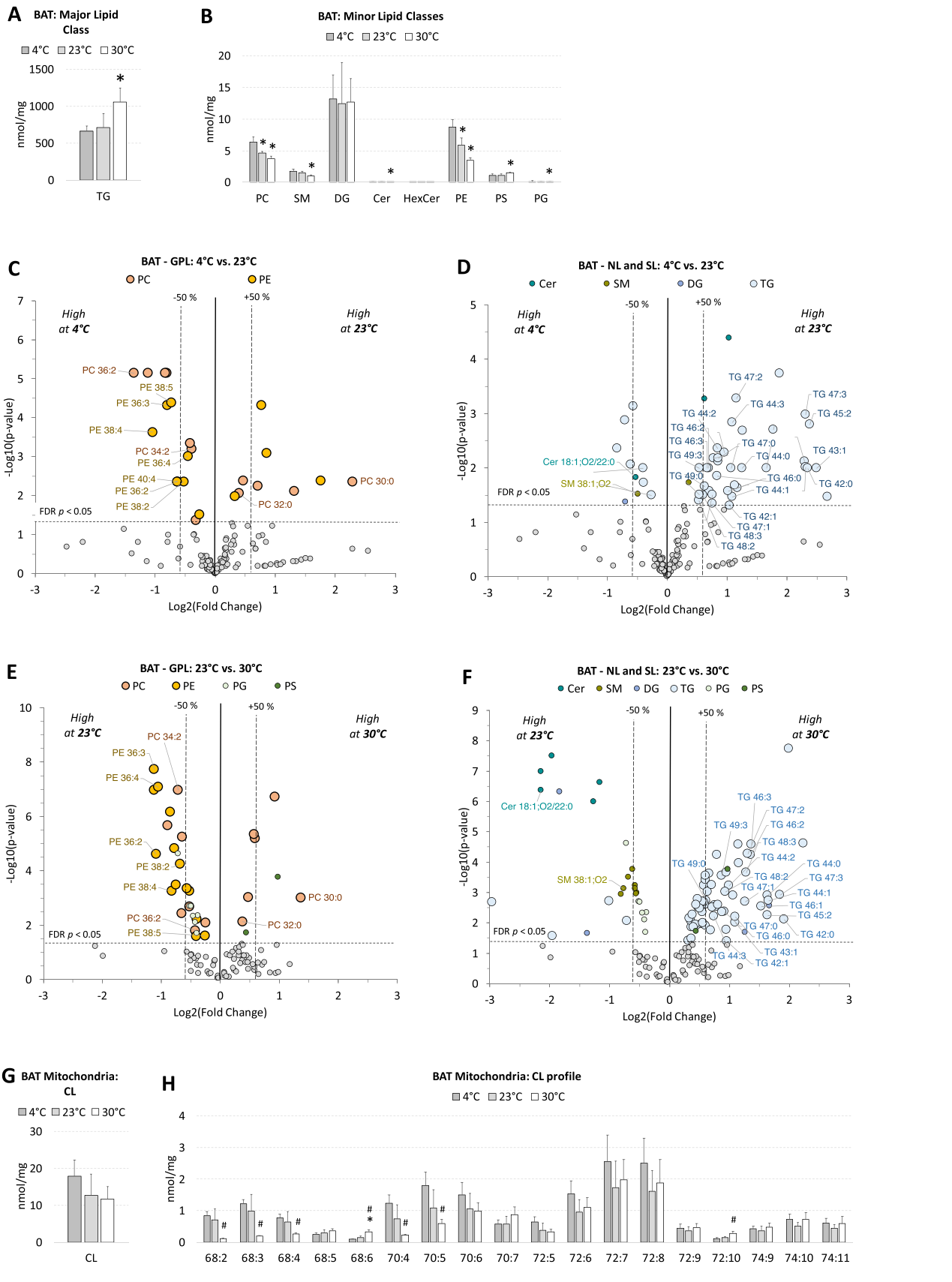


*(caption on next page)*

**Fig. 2. Cold exposure increases polyunsaturated PE and PC in BAT of mice**
**(A)** Concentrations of major and **(B)** minor lipid classes at cold (4 °C), room temperature (23 °C) and thermoneutrality (30 °C). *p < 0.05 indicates a significant difference between groups, determined by two-sided Student's t-test. Shown are means +SD from BAT of n = 9 (4 °C), n = 9 (23 °C) and n = 12 (30 °C). Volcano plots show Log2 fold changes of lipids in BAT, whose concentrations are significantly different between 4 °C vs. 23 °C including **(C)** GPL, **(D)** NL and SL; and 23 °C vs. 30 °C including **(E)** GPL, **(F)** NL and SL. Only lipids that were significantly altered and showed the same direction of regulation in both comparisons are labeled in the volcano plots. Large dots indicate lipid species from the major lipid classes. p < 0.05 is indicated after correction for multiple testing by controlling for false discovery rate. **(G)** Concentrations of total CL and **(H)** CL species of mitochondria isolated from BAT of mice housed at 4 °C, 23 °C or 30 °C. *p < 0.05 indicates a significant difference for the comparisons 4 °C vs. 23 °C or 23 °C vs. 30 °C, #p < 0.05 indicates a significant difference for the comparisons 4 °C vs. 30 °C determined by two-sided Student's t-test. Shown are means +SD from *n* = 3 mitochondrial samples per housing temperature.

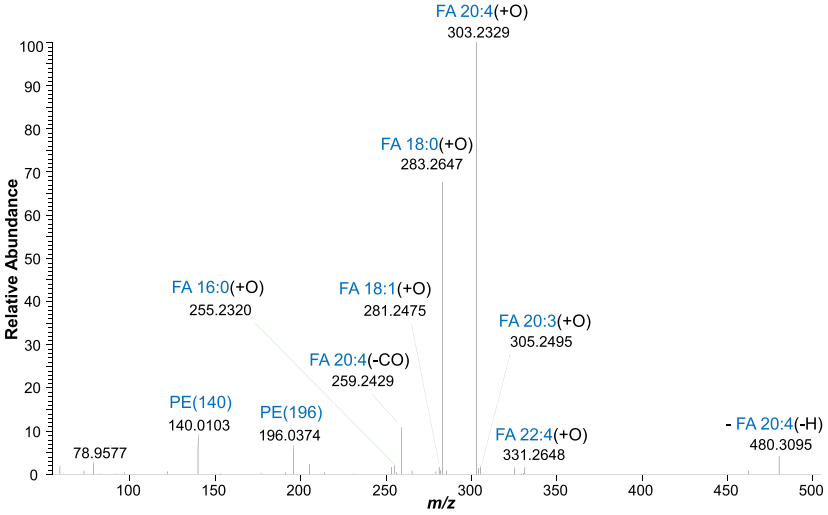


**Fig. 3. Product ion spectrum of PE 38:4 in liver.** Electrospray ionization tandem mass spectrometry showing the product ions obtained following collisional activation of PE 38:4 $[M\text{-}H]^-$ (*m/z* 766.5392) of a representative liver sample obtained from mice housed at 4 °C.

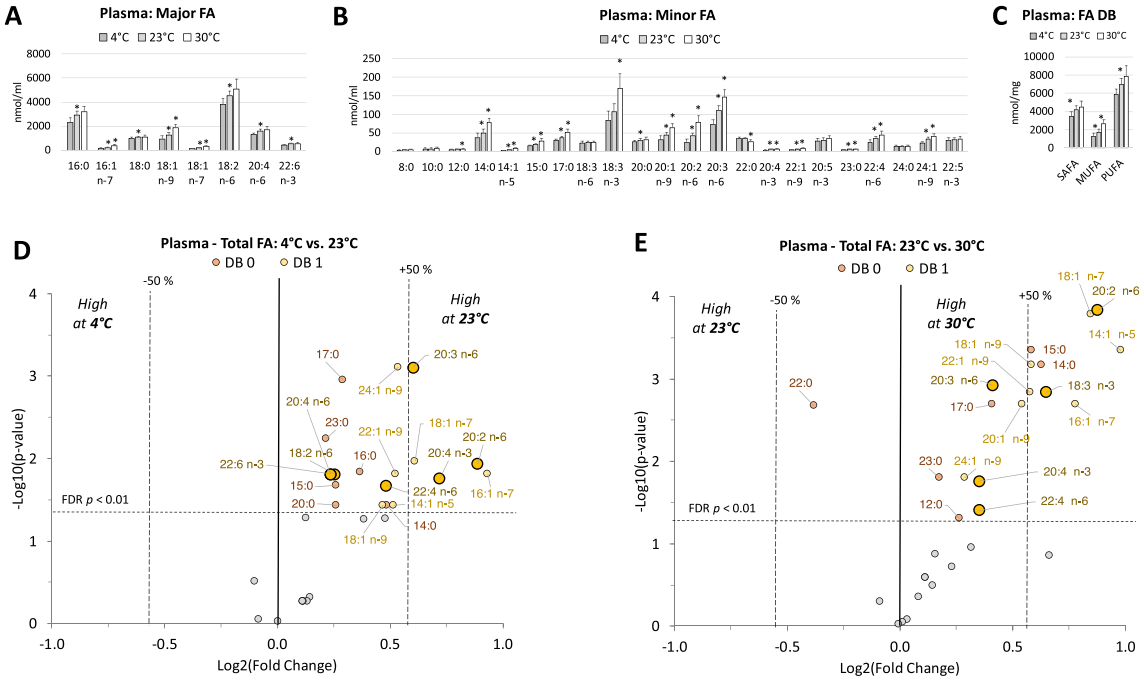


**Fig. 4. Plasma polyunsaturated FA 20:2 n-6, FA 20:3 n-6, FA 20:4 n-3, FA 22:4 n-6 are markedly reduced in cold-exposed mice.**
**(A)** Circulating concentrations of major and **(B)** minor fatty acids at cold (4 °C), room temperature (23 °C) and thermoneutrality (30 °C). *p < 0.05 indicates a significant difference between groups, determined by a two-sided Student's t-test. Shown are means +SD from plasma of n = 9 (4 °C), *n* = 8 (23 °C) and *n* = 10 (30 °C). Volcano plots show Log2 fold changes of circulating fatty acids, whose concentrations are significantly different between **(C)** 4 °C vs. 23 °C and **(D)** 23 °C vs. 30 °C. Large dots indicate major FA species. p < 0.05 is indicated after correction for multiple testing by controlling for false discovery rate.

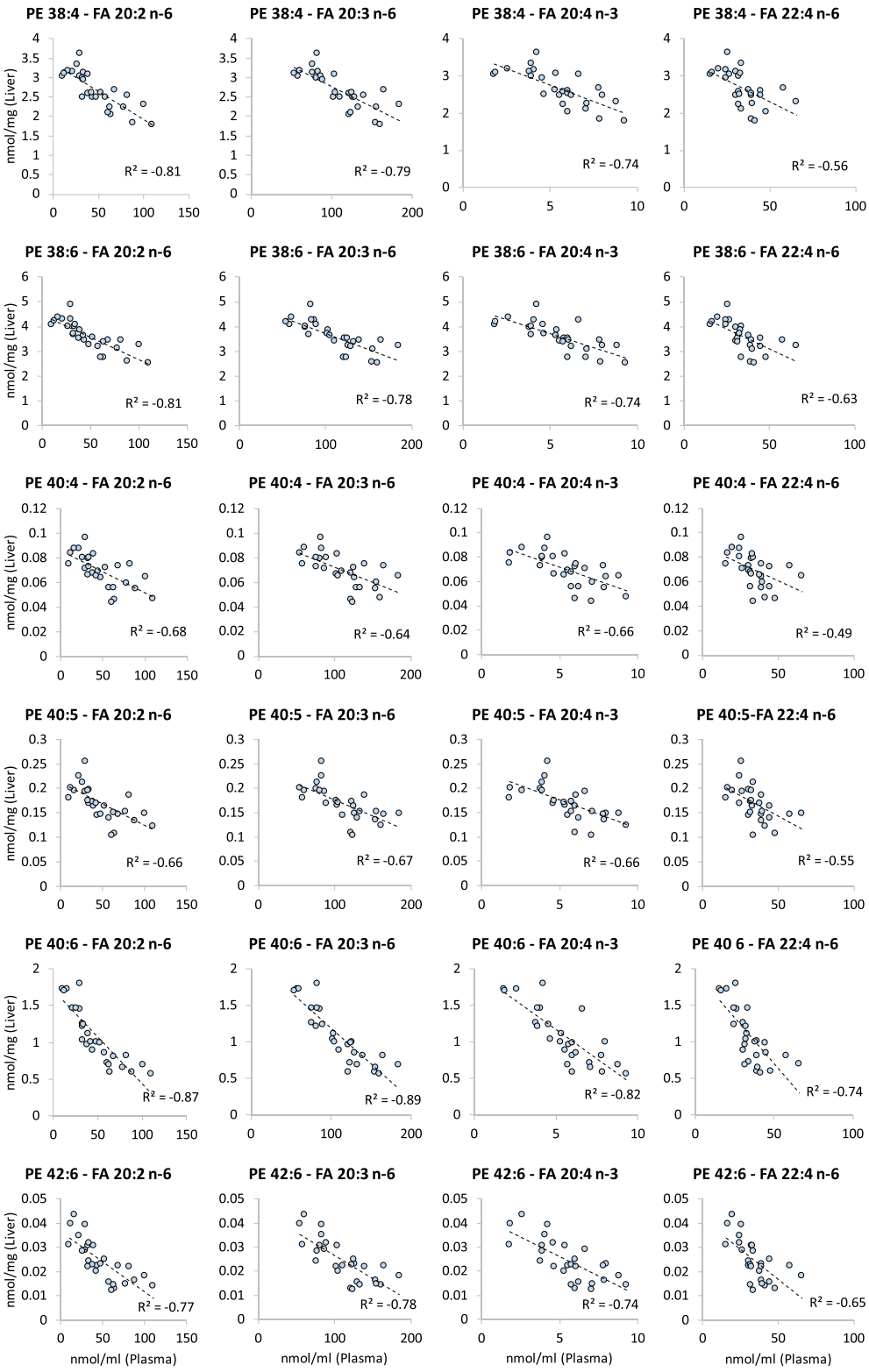


**Fig. 5. Circulating PUFAs negatively correlate with increased polyunsaturated PE species in liver**
Correlation of significantly reduced plasma PUFAs (FA 20:2, FA 20:3, FA 20:4, FA 22:4) with polyunsaturated hepatic PE species, that were significantly increased by colder temperatures in liver (PE 38:4, 38:6, 40:4, 40:5, 40:6, 42:6). $R^2$ indicate Pearson's correlation coefficients.

malondialdehyde and reactive oxygen species and indicators for liver damage like serum alanine aminotransferase and aspartate aminotransferase levels are elevated, which can be prevented by pretreatment with ferroptosis inhibitor liproystatin-1 [52]. In our study, PE 18:0_20:4 was increased by cold in liver and BAT. FA 20:4 is highly susceptible to radical-caused damage and peroxidation [53]. Interestingly, we have recently linked ferroptosis with PE metabolism in prostate cancer cells, as punic acid (c9, t11, c13-FA 18:3), an isomer of conjugated linolenic acid, induces both ferroptosis as well as PUFA-containing PE synthesis and remodeling [54].

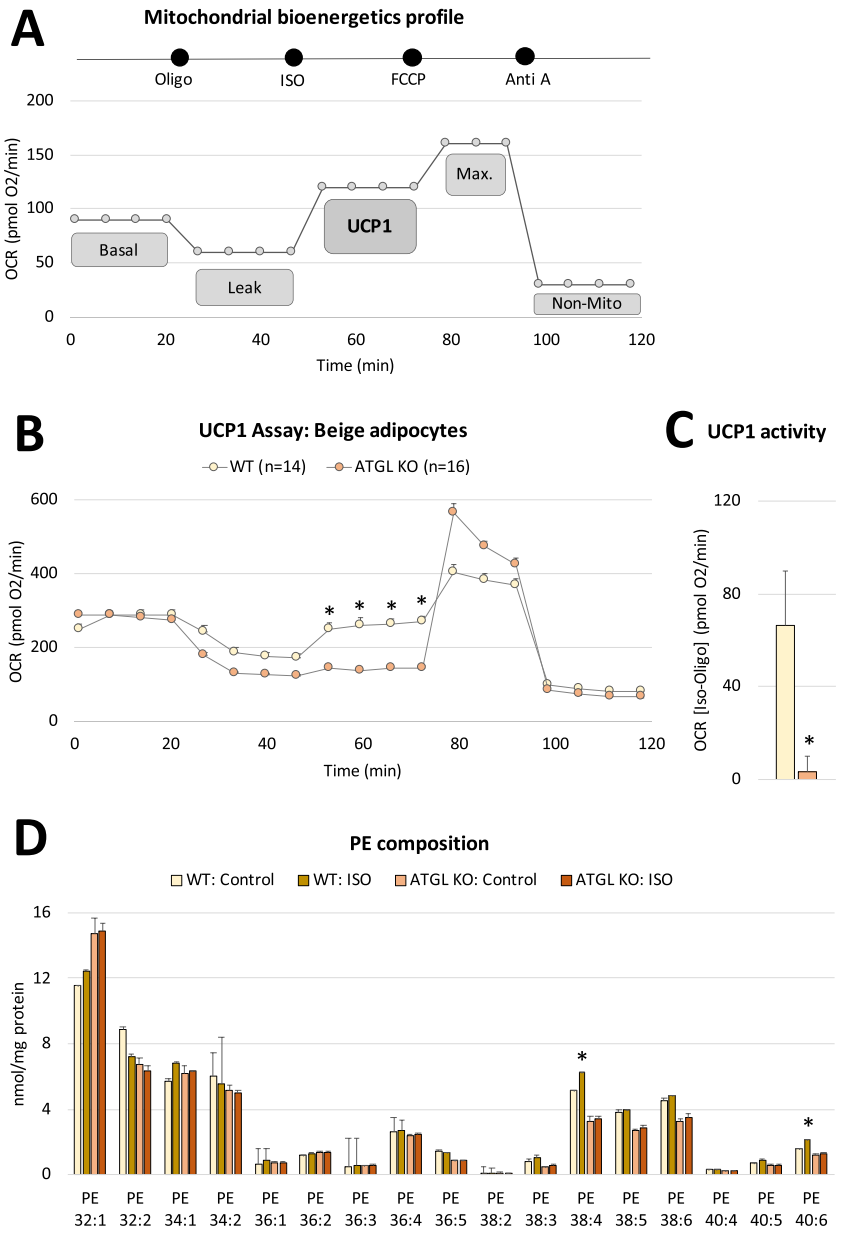


**Fig. 6. Cellular lipolysis induces UCP1 and increases PE 38:4 and PE 40:6 in beige wildtype adipocytes**
**(A)** Microplate-based respirometry assay used to profile UCP1 activity in primary beige adipocytes. Oxygen consumption rate (OCR) was measured as [a] basal respiration, followed by [b] proton leak-linked respiration induced by oligomycin, [c] UCP1-dependent respiration after ISO, [d] maximal respiratory capacity after FCCP, [e] non-mitochondrial $O_2$ consumption after Anti A injection. **(B)** Mitochondrial bioenergetic profile of primary beige adipocytes isolated from iWAT of WT and ATGL KO mice; shown are means +SEM of $n = 14$ (WT) and $n = 16$ (ATGL KO). **(C)** UCP1 activity calculated by subtracting the OCR at [b] (Oligo) from [c] (ISO) determined in b; shown are means +SD. $p < 0.05$ after a two-sided Student's t-test. **(E)** PE profile of primary beige adipocytes isolated from iWAT of WT or ATGL KO mice treated with 0.5 μM ISO or ethanol (Control) for 30 min; shown are means +SD of n = 3 for each condition. *$p < 0.05$ indicates a significant difference between WT and ATGL KO cells after ISO treatment **(B—C)** and between control and ISO-treated WT or ATGL KO cells **(D)** determined by a two-sided Student's t-test.

For quantitative lipidomic analysis of liver and BAT samples, we used flow injection analysis mass spectrometry. To improve the sensitivity of phospholipid quantification in BAT, it's excess TG content was depleted prior to analysis. This strategy should cover the vast majority of lipid species from the major lipid classes, although very low abundant species may not be detected due to sensitivity limitations inherent to direct infusion. To the best of our knowledge, liver lipidomic data after long term cold exposure are not yet available. Lynes and colleagues reported that PG and CL metabolism in WAT and BAT are activated when mice are housed for one week at 4 °C compared to animals at 30 °C [55]. The levels of some C16 FA- and C18 FA-containing PG and CL species with 2–6 double bonds were found to be altered, although total amounts of PG and CL remained unchanged. In our study, hepatic concentrations of CL containing 2 to 12 double bonds, like CL 36:4_40:8, were increased in both comparisons **[I]** and **[II]**. But, total CL levels were solely slightly higher in comparison **[I]** (by ≈ 10 %) and similar in **[II]**. Human cold exposure trials focus on plasma lipids with mixed results. While some studies indicate metabolism of FFA to TG after a 1–2 h-long exposure to mild cold [21,56], others have detected no changes in circulating TG in response to cold [57,58]. Translation of results from short to long term cold exposure studies is limited. Cold stimuli in the range of hours give insights into acute metabolic changes, while longer term cold exposure in the range of days allows the investigation of accumulated lipidomic alterations in peripheral tissues. When comparing lipidomic

investigations in mice with human studies, it has to be considered that lipoprotein metabolism differs [59,60]. Mice lack cholesterol ester transfer protein (CETP) [61] and comprise another adipose tissue composition than humans [18,20,62,63].

Our data indicate a cold-induced de novo PE synthesis as well as PE remodeling in liver and BAT, because both total PE amounts as well as its species composition were altered in comparisons **[I]** and **[II]**. Particularly PE containing PUFA in their acyl chains were elevated following cold exposure. In line with this finding, a previous study showed that housing mice at 4 °C for 3 days activates gene expression related to glycerophospholipid synthesis, FA elongation and remodeling of FA 18:2-containing PE in BAT [64]. The rationale for FFA being metabolized to complex lipids such as PE after lipolysis might be that accumulated non-esterified FA are lipotoxic, leading to apoptosis and ultimately metabolic disease [65]. We hypothesize that lipolysis-derived FFA are distributed between organs for further consumption and metabolism. This includes activating UCP1 and fueling beta-oxidation in BAT [7,8]; beta-oxidation in liver [66]; metabolism to acylcarnitines and TG in liver [22,23,67]; metabolism to PG and CL in BAT and WAT [55]; and, as reported here, incorporation into PE in liver and PE and PC in BAT.

Several potential sources of PUFA metabolized to PE in the liver and BAT are feasible: (1) FA released via ATGL within these tissues. ATGL has been shown to exhibit activity towards TG esterified with unsaturated FA [68]. In line, our data show that ISO-induced metabolism of PE 38:4 and 40:6 is impaired using primary beige ATGL KO adipocytes. (2) ATGL-mediated FA release in WAT controls PUFA flux towards the liver and BAT. Our data show that plasma PUFA negatively correlate with hepatic and BAT PUFA-containing PE levels. Moreover, loss of ATGL in WAT is associated with reduced unsaturated FAs in the circulation [68]. And (3), dietary PUFA reaching the liver and BAT after intestinal uptake via the blood stream. In mice with a BAT-specific ATGL KO, non-shivering thermogenesis via UCP1 can be fueled by dietary FA during feeding or WAT lipolysis during fasting [69].

The reason why PUFA are preferentially integrated into GPL, rather than neutral lipids, may be explained by their specific physical and steric properties. In contrast to saturated FA, which are basically straight molecules, PUFA are characterized by a remarkable structural flexibility. Their carbon chains can freely rotate after the double bonds [70]. This leads to a larger conformational landscape, which is most likely rather available in GPL, like PE and PC, containing only two acyl chains, than TG, having three dense acyl chains, bound to its backbone. Indeed, we could demonstrate previously that the FA incorporation into complex lipids depends on their steric properties [71]. Trans-9,trans-11-conjugated linoleic acid (t9, t11-FA 18:2), which is a relatively straight molecule (comparable to saturated FA) due to its planar and rigid conjugated double bond system, is primarily incorporated into neutral lipids like TG. In contrast, cis-9,trans-11-conjugated linoleic acid (c9, t11-FA 18:2), which is a curved and more spacious molecule because of its cis-double bond, is rather incorporated in PC and PE in human macrophages. The question of why, at least in liver, PUFA are rather incorporated into PE than PC might be of interest for future investigations. It could be related to their different headgroup sizes. The PE headgroup is considerably smaller than that of PC (38$Å^2$ compared with 50 $Å^2$) since its nitrogen atom is bound to three hydrogen atoms, whereas the nitrogen atom of the PC headgroup is bound to three methyl groups [72,73]. As consequence, PE molecules tend to have more cylindrical shapes, while PCs are more conical [70].

The reasons why beta-adrenergic stimulation and/or PUFA promote biosynthesis of PE in liver and PE and PC in BAT could be diverse: (1) A metabolic regulation of GPL synthesis: An increasing substrate (i.e. PUFA) availability might drive GPL synthesis, as previously observed in cells [71,74]. (2) A transcriptional regulation of genes relevant for GPL synthesis: PUFA could activate PPAR alpha, which in turn inhibits liver X receptor (LXR), thereby repressing the transcription of Pcyt2, encoding CTP:phosphoethanolamine cytidylyltransferase as the main regulatory enzyme in de novo PE biosynthesis [75,76]. (3) A post-translational activation of enzymes necessary for GPL synthesis: Choline-phosphate cytidyltransferase (CCT), the key enzyme of PC synthesis, is translocated from its inactive soluble form to a membrane-associated active form when the membrane's physicochemical properties change, i.e. its curvature [77]. The membrane's PUFA content essentially shapes its physicochemical properties, including curvature [70]. Molecular dynamic simulations with liposomes showed that acyl chain polyunsaturation in PC, PE and PS makes cellular membranes more flexible and facilitates vesicle formation, necessary in synaptic membranes undergoing super-fast endocytosis [78]. Also, the degree of unsaturation in PC systematically accelerates the dynamics of the phosphocholine headgroups and glycerol backbones as well as PC's rotational capacity [79]. Though, it is unclear whether the increase in the PUFA containing GPL fraction determined here in liver and BAT is sufficient to change membrane curvature and promote CCT translocation.

In summary, we demonstrate that long-term cold exposure increases concentrations of PE in mouse liver and BAT, proposing an elevated synthesis and metabolism. Particularly, PE species containing PUFA, most likely taken up from the circulation, were increased after cold-induced lipolysis. We conclude that free PUFA in liver and BAT are preferentially incorporated into PE to prevent lipotoxicity induced by accumulation of non-esterified FA.

Supplementary data to this article can be found online at https://doi.org/10.1016/j.bbalip.2024.159562.

## CRediT authorship contribution statement

**Maria Soledad Hidrobo:** Writing – review & editing, Visualization, Validation, Methodology, Investigation, Data curation. **Marcus Höring:** Writing – review & editing, Validation, Methodology, Investigation, Data curation. **Sarah Brunner:** Writing – review & editing, Methodology, Investigation. **Gerhard Liebisch:** Writing – review & editing, Resources, Methodology, Investigation. **Sabine Schweizer:** Investigation. **Martin Klingenspor:** Investigation. **Renate Schreiber:** Writing – review & editing, Resources, Methodology, Investigation. **Rudolf Zechner:** Resources, Investigation. **Ralph Burkhardt:** Writing – review & editing, Resources, Investigation. **Josef Ecker:** Writing – review & editing, Writing – original draft, Visualization, Validation, Supervision, Resources, Project administration, Investigation, Funding acquisition, Data curation, Conceptualization.

## Declaration of competing interest

The authors declare that they have no known competing financial interests or personal relationships that could have appeared to influence the work reported in this paper.

## Data availability

Lipidomic data are enclosed as Supplementary Data 1.

*Acknowledgements*

We thank Doreen Mueller, Renate Kick and Dagmar Alzinger for excellent technical assistance.

*Funding sources*

This work was funded by the Deutsche Forschungsgemeinschaft (DFG, German Research Foundation) – project numbers 446175916 (EC 453/4–1) and 395357507 (SFB 1371, Microbiome Signatures).

*Author contributions*

J.E. conceived and designed the experiments; M.S.H., M.H., S.S., G. L., R.S., S.B. performed the experiments; J.E., M.S.H., M.H., S.S., G.L., R. S. analyzed the data; J.E., G.L., M.K., R.Z., R.B. contributed materials/ analysis tools; J.E., M.S.H. wrote the paper.

## References


[1] E.J. Benjamin, M.J. Blaha, S.E. Chiuve, M. Cushman, S.R. Das, R. Deo, S.D. de Ferranti, J. Floyd, M. Fornage, C. Gillespie, C.R. Isasi, M.C. Jimenez, L.C. Jordan, S. E. Judd, D. Lackland, J.H. Lichtman, L. Lisabeth, S. Liu, C.T. Longenecker, R. H. Mackey, K. Matsushita, D. Mozaffarian, M.E. Mussolino, K. Nasir, R.W. Neumar, L. Palaniappan, D.K. Pandey, R.R. Thiagarajan, M.J. Reeves, M. Ritchey, C. J. Rodriguez, G.A. Roth, W.D. Rosamond, C. Sasson, A. Towfighi, C.W. Tsao, M. B. Turner, S.S. Virani, J.H. Voeks, J.Z. Willey, J.T. Wilkins, J.H. Wu, H.M. Alger, S. S. Wong, P. Muntner, C. American Heart Association Statistics, S. Stroke Statistics, Heart Disease and Stroke Statistics-2017 Update: A Report From the American Heart Association, Circulation 135 (10) (2017) e146–e603.

[2] M.J. Hanssen, J. Hoeks, B. Brans, A.A. van der Lans, G. Schaart, J.J. van den Driessche, J.A. Jorgensen, M.V. Boekschoten, M.K. Hesselink, B. Havekes, S. Kersten, F.M. Mottaghy, W.D. van Marken Lichtenbelt, P. Schrauwen, Short-term cold acclimation improves insulin sensitivity in patients with type 2 diabetes mellitus, Nat. Med. 21 (8) (2015) 863–865.

[3] T. Yoneshiro, S. Aita, M. Matsushita, T. Kayahara, T. Kameya, Y. Kawai, T. Iwanaga, M. Saito, Recruited brown adipose tissue as an antiobesity agent in humans, J. Clin. Invest. 123 (8) (2013) 3404–3408.

[4] M.F. Shih, P.V. Taberner, Selective activation of brown adipocyte hormone-sensitive lipase and cAMP production in the mouse by beta 3-adrenoceptor agonists, Biochem. Pharmacol. 50 (5) (1995) 601–608.

[5] C.M. Jenkins, D.J. Mancuso, W. Yan, H.F. Sims, B. Gibson, R.W. Gross, Identification, cloning, expression, and purification of three novel human calcium-independent phospholipase A2 family members possessing triacylglycerol lipase and acylglycerol transacylase activities, J. Biol. Chem. 279 (47) (2004) 48968–48975.

[6] H. Shin, Y. Ma, T. Chanturiya, Q. Cao, Y. Wang, A.K.G. Kadegowda, R. Jackson, D. Rumore, B. Xue, H. Shi, O. Gavrilova, L. Yu, Lipolysis in Brown adipocytes is not essential for cold-induced thermogenesis in mice, Cell Metab. 26 (5) (2017) 764–777.

[7] P.G. Crichton, Y. Lee, E.R. Kunji, The molecular features of uncoupling protein 1 support a conventional mitochondrial carrier-like mechanism, Biochimie 134 (2017) 35–50.

[8] R.M. Locke, E. Rial, I.D. Scott, D.G. Nicholls, Fatty acids as acute regulators of the proton conductance of hamster brown-fat mitochondria, Eur. J. Biochem. 129 (2) (1982) 373–380.

[9] K.D. Garlid, D.E. Orosz, M. Modriansky, S. Vassanelli, P. Jezek, On the mechanism of fatty acid-induced proton transport by mitochondrial uncoupling protein, J. Biol. Chem. 271 (5) (1996) 2615–2620.

[10] M. Klingenberg, S.G. Huang, Structure and function of the uncoupling protein from brown adipose tissue, Biochim. Biophys. Acta 1415 (2) (1999) 271–296.

[11] A.M. Bertholet, L. Kazak, E.T. Chouchani, M.G. Bogaczynska, I. Paranjpe, G. L. Wainwright, A. Betourne, S. Kajimura, B.M. Spiegelman, Y. Kirichok, Mitochondrial patch clamp of beige adipocytes reveals UCP1-positive and UCP1-negative cells both exhibiting futile creatine cycling, Cell Metab. 25 (4) (2017) 811–822 e4.

[12] V. Beck, M. Jaburek, T. Demina, A. Rupprecht, R.K. Porter, P. Jezek, E.E. Pohl, Polyunsaturated fatty acids activate human uncoupling proteins 1 and 2 in planar lipid bilayers, FASEB J. 21 (4) (2007) 1137–1144.

[13] A. Fedorenko, P.V. Lishko, Y. Kirichok, Mechanism of fatty-acid-dependent UCP1 uncoupling in brown fat mitochondria, Cell 151 (2) (2012) 400–413.

[14] D.P. Blondin, S.M. Labbe, H.C. Tingelstad, C. Noll, M. Kunach, S. Phoenix, B. Guerin, E.E. Turcotte, A.C. Carpentier, D. Richard, F. Haman, Increased brown adipose tissue oxidative capacity in cold-acclimated humans, J. Clin. Endocrinol. Metab. 99 (3) (2014) E438–E446.

[15] A.M. Cypess, S. Lehman, G. Williams, I. Tal, D. Rodman, A.B. Goldfine, F.C. Kuo, E. L. Palmer, Y.H. Tseng, A. Doria, G.M. Kolodny, C.R. Kahn, Identification and importance of brown adipose tissue in adult humans, N. Engl. J. Med. 360 (15) (2009) 1509–1517.

[16] A.M. Cypess, L.S. Weiner, C. Roberts-Toler, E. Franquet Elia, S.H. Kessler, P. A. Kahn, J. English, K. Chatman, S.A. Trauger, A. Doria, G.M. Kolodny, Activation of human brown adipose tissue by a beta3-adrenergic receptor agonist, Cell Metab. 21 (1) (2015) 33–38.

[17] W.D. van Marken Lichtenbelt, J.W. Vanhommerig, N.M. Smulders, J.M. Drossaerts, G.J. Kemerink, N.D. Bouvy, P. Schrauwen, G.J. Teule, Cold-activated brown adipose tissue in healthy men, N. Engl. J. Med. 360 (15) (2009) 1500–1508.

[18] B.P. Leitner, S. Huang, R.J. Brychta, C.J. Duckworth, A.S. Baskin, S. McGehee, I. Tal, W. Dieckmann, G. Gupta, G.M. Kolodny, K. Pacak, P. Herscovitch, A. M. Cypess, K.Y. Chen, Mapping of human brown adipose tissue in lean and obese young men, Proc. Natl. Acad. Sci. USA 114 (32) (2017) 8649–8654.

[19] V. Ouellet, A. Routhier-Labadie, W. Bellemare, L. Lakhal-Chaieb, E. Turcotte, A. C. Carpentier, D. Richard, Outdoor temperature, age, sex, body mass index, and diabetic status determine the prevalence, mass, and glucose-uptake activity of 18F-FDG-detected BAT in humans, J. Clin. Endocrinol. Metab. 96 (1) (2011) 192–199.

[20] A. Vitali, I. Murano, M.C. Zingaretti, A. Frontini, D. Ricquier, S. Cinti, The adipose organ of obesity-prone C57BL/6J mice is composed of mixed white and brown adipocytes, J. Lipid Res. 53 (4) (2012) 619–629.

[21] M.E. Straat, L. Jurado-Fasoli, Z. Ying, K.J. Nahon, L.G.M. Janssen, M.R. Boon, G. F. Grabner, S. Kooijman, R. Zimmermann, M. Giera, P.C.N. Rensen, B. Martinez-Tellez, Cold exposure induces dynamic changes in circulating triacylglycerol species, which is dependent on intracellular lipolysis: a randomized cross-over trial, EBioMedicine 86 (2022) 104349.

[22] J. Simcox, G. Geoghegan, J.A. Maschek, C.L. Bensard, M. Pasquali, R. Miao, S. Lee, L. Jiang, I. Huck, E.E. Kershaw, A.J. Donato, U. Apte, N. Longo, J. Rutter, R. Schreiber, R. Zechner, J. Cox, C.J. Villanueva, Global analysis of plasma lipids identifies liver-derived acylcarnitines as a fuel source for Brown fat thermogenesis, Cell Metab. 26 (3) (2017) 509–522 e6.

[23] R. Jain, G. Wade, I. Ong, B. Chaurasia, J. Simcox, Determination of tissue contributions to the circulating lipid pool in cold exposure via systematic assessment of lipid profiles, J. Lipid Res. 63 (7) (2022) 100197.

[24] S. Brunner, M. Horing, G. Liebisch, S. Schweizer, J. Scheiber, P. Giansanti, M. Hidrobo, S. Hermeling, J. Oeckl, N. Prudente de Mello, F. Perocchi, C. Seeliger, A. Strohmeyer, M. Klingenspor, J. Plagge, B. Kuster, R. Burkhardt, K.P. Janssen, J. Ecker, Mitochondrial lipidomes are tissue specific - low cholesterol contents relate to UCP1 activity, Life Sci Alliance 7 (8) (2024).

[25] G. Haemmerle, A. Lass, R. Zimmermann, G. Gorkiewicz, C. Meyer, J. Rozman, G. Heldmaier, R. Maier, C. Theussl, S. Eder, D. Kratky, E.F. Wagner, M. Klingenspor, G. Hoefler, R. Zechner, Defective lipolysis and altered energy metabolism in mice lacking adipose triglyceride lipase, Science 312 (5774) (2006) 734–737.

[26] J. Oeckl, A. Bast-Habersbrunner, T. Fromme, M. Klingenspor, Y. Li, Isolation, culture, and functional analysis of murine thermogenic adipocytes, STAR Protoc 1 (3) (2020) 100118.

[27] S. Schweizer, G. Liebisch, J. Oeckl, M. Hoering, C. Seeliger, C. Schiebel, M. Klingenspor, J. Ecker, The lipidome of primary murine white, brite, and brown adipocytes-impact of beta-adrenergic stimulation, PLoS Biol. 17 (8) (2019) e3000412.

[28] G. Liebisch, E. Fahy, J. Aoki, E.A. Dennis, T. Durand, C.S. Ejsing, M. Fedorova, I. Feussner, W.J. Griffiths, H. Kofeler, A.H. Merrill Jr., R.C. Murphy, V. B. O'Donnell, O. Oskolkova, S. Subramaniam, M.J.O. Wakelam, F. Spener, Update on LIPID MAPS classification, nomenclature, and shorthand notation for MS-derived lipid structures, J. Lipid Res. 61 (12) (2020) 1539–1555.

[29] E.G. Bligh, W.J. Dyer, A rapid method of total lipid extraction and purification, Can. J. Biochem. Physiol. 37 (8) (1959) 911–917.

[30] G. Liebisch, B. Lieser, J. Rathenberg, W. Drobnik, G. Schmitz, High-throughput quantification of phosphatidylcholine and sphingomyelin by electrospray ionization tandem mass spectrometry coupled with isotope correction algorithm, Biochim. Biophys. Acta 1686 (1–2) (2004) 108–117.

[31] G. Liebisch, M. Binder, R. Schifferer, T. Langmann, B. Schulz, G. Schmitz, High throughput quantification of cholesterol and cholesteryl ester by electrospray ionization tandem mass spectrometry (ESI-MS/MS), Biochim. Biophys. Acta 1761 (1) (2006) 121–128.

[32] G. Liebisch, W. Drobnik, B. Lieser, G. Schmitz, High-throughput quantification of lysophosphatidylcholine by electrospray ionization tandem mass spectrometry, Clin. Chem. 48 (12) (2002) 2217–2224.

[33] V. Matyash, G. Liebisch, T.V. Kurzchalia, A. Shevchenko, D. Schwudke, Lipid extraction by methyl-tert-butyl ether for high-throughput lipidomics, J. Lipid Res. 49 (5) (2008) 1137–1146.

[34] G. Liebisch, W. Drobnik, M. Reil, B. Trumbach, R. Arnecke, B. Olgemoller, A. Roscher, G. Schmitz, Quantitative measurement of different ceramide species from crude cellular extracts by electrospray ionization tandem mass spectrometry (ESI-MS/MS), J. Lipid Res. 40 (8) (1999) 1539–1546.

[35] K.A. Zemski Berry, R.C. Murphy, Electrospray ionization tandem mass spectrometry of glycerophosphoethanolamine plasmalogen phospholipids, J. Am. Soc. Mass Spectrom. 15 (10) (2004) 1499–1508.

[36] M. Scherer, G. Schmitz, G. Liebisch, Simultaneous quantification of cardiolipin, bis (monoacylglycero)phosphate and their precursors by hydrophilic interaction LC-MS/MS including correction of isotopic overlap, Anal. Chem. 82 (21) (2010) 8794–8799.

[37] M. Horing, C.S. Ejsing, S. Krautbauer, V.M. Ertl, R. Burkhardt, G. Liebisch, Accurate quantification of lipid species affected by isobaric overlap in Fourier-transform mass spectrometry, J. Lipid Res. 62 (2021) 100050.

[38] M. Horing, K. Ekroos, P.R.S. Baker, L. Connell, S.C. Stadler, R. Burkhardt, G. Liebisch, Correction of isobaric overlap resulting from sodiated ions in lipidomics, Anal. Chem. 92 (16) (2020) 10966–10970.

[39] M. Horing, C.S. Ejsing, M. Hermansson, G. Liebisch, Quantification of cholesterol and cholesteryl ester by direct flow injection high-resolution fourier transform mass spectrometry utilizing species-specific response factors, Anal. Chem. 91 (5) (2019) 3459–3466.

[40] J. Ecker, M. Scherer, G. Schmitz, G. Liebisch, A rapid GC-MS method for quantification of positional and geometric isomers of fatty acid methyl esters, J. Chromatogr. B Anal. Technol. Biomed. Life Sci. 897 (2012) 98–104.

[41] A. Kindt, G. Liebisch, T. Clavel, D. Haller, G. Hormannsperger, H. Yoon, D. Kolmeder, A. Sigruener, S. Krautbauer, C. Seeliger, A. Ganzha, S. Schweizer, R. Morisset, T. Strowig, H. Daniel, D. Helm, B. Kuster, J. Krumsiek, J. Ecker, The gut microbiota promotes hepatic fatty acid desaturation and elongation in mice, Nat. Commun. 9 (1) (2018) 3760.

[42] J. Ecker, E. Benedetti, A.S.D. Kindt, M. Horing, M. Perl, A.C. Machmuller, A. Sichler, J. Plagge, Y. Wang, S. Zeissig, A. Shevchenko, R. Burkhardt, J. Krumsiek, G. Liebisch, K.P. Janssen, The colorectal cancer lipidome:

identification of a robust tumor-specific lipid species signature, Gastroenterology 161 (3) (2021) 910–923.
[43] J.M. Johnson, A.D. Peterlin, E. Balderas, E.G. Sustarsic, J.A. Maschek, M.J. Lang, A. Jara-Ramos, V. Panic, J.T. Morgan, C.J. Villanueva, A. Sanchez, J. Rutter, I. J. Lodhi, J.E. Cox, K.H. Fisher-Wellman, D. Chaudhuri, Z. Gerhart-Hines, K. Funai, Mitochondrial phosphatidylethanolamine modulates UCP1 to promote brown adipose thermogenesis, Sci. Adv. 9 (8) (2023) eade7864.
[44] G. van Meer, D.R. Voelker, G.W. Feigenson, Membrane lipids: where they are and how they behave, Nat. Rev. Mol. Cell Biol. 9 (2) (2008) 112–124.
[45] Y. Li, T. Fromme, M. Klingenspor, Meaningful respirometric measurements of UCP1-mediated thermogenesis, Biochimie 134 (2017) 56–61.
[46] Y. Li, T. Fromme, S. Schweizer, T. Schottl, M. Klingenspor, Taking control over intracellular fatty acid levels is essential for the analysis of thermogenic function in cultured primary brown and brite/beige adipocytes, EMBO Rep. 15 (10) (2014) 1069–1076.
[47] M. Rosenwald, A. Perdikari, T. Rulicke, C. Wolfrum, Bi-directional interconversion of brite and white adipocytes, Nat. Cell Biol. 15 (6) (2013) 659–667.
[48] J. Wu, P. Boström, Lauren M. Sparks, L. Ye, Jang H. Choi, A.-H. Giang, M. Khandekar, Kirsi A. Virtanen, P. Nuutila, G. Schaart, K. Huang, H. Tu, Wouter D. van Marken, J. Lichtenbelt, S. Hoeks, P. Schrauwen Enerbäck, Bruce M. Spiegelman, Beige adipocytes are a distinct type of thermogenic fat cell in mouse and human, Cell 150 (2) (2012) 366–376.
[49] F. Vialard, M. Olivier, Thermoneutrality and immunity: how does cold stress affect disease? Front. Immunol. 11 (2020) 588387.
[50] C.J. Gordon, The mouse thermoregulatory system: its impact on translating biomedical data to humans, Physiol. Behav. 179 (2017) 55–66.
[51] X. Jiang, B.R. Stockwell, M. Conrad, Ferroptosis: mechanisms, biology and role in disease, Nat. Rev. Mol. Cell Biol. 22 (4) (2021) 266–282.
[52] Y. Huang, K. Xiong, A. Wang, Z. Wang, Q. Cui, H. Xie, T. Yang, X. Fan, W. Jiang, X. Tan, Q. Huang, Cold stress causes liver damage by inducing ferroptosis through the p38 MAPK/Drp1 pathway, Cryobiology 113 (2023) 104563.
[53] H. Yin, L. Xu, N.A. Porter, Free radical lipid peroxidation: mechanisms and analysis, Chem. Rev. 111 (10) (2011) 5944–5972.
[54] P. Vermonden, M. Martin, K. Glowacka, I. Neefs, J. Ecker, M. Horing, G. Liebisch, C. Debier, O. Feron, Y. Larondelle, Phospholipase PLA2G7 is complementary to GPX4 in mitigating punicic-acid-induced ferroptosis in prostate cancer cells, iScience 27 (5) (2024) 109774.
[55] M.D. Lynes, F. Shamsi, E.G. Sustarsic, L.O. Leiria, C.H. Wang, S.C. Su, T.L. Huang, F. Gao, N.R. Narain, E.Y. Chen, A.M. Cypess, T.J. Schulz, Z. Gerhart-Hines, M. A. Kiebish, Y.H. Tseng, Cold-activated lipid dynamics in adipose tissue highlights a role for cardiolipin in thermogenic metabolism, Cell Rep. 24 (3) (2018) 781–790.
[56] G. Hoeke, K.J. Nahon, L.E.H. Bakker, S.S.C. Norkauer, D.L.M. Dinnes, M. Kockx, L. Lichtenstein, D. Drettwan, A. Reifel-Miller, T. Coskun, P. Pagel, F. Romijn, C. M. Cobbaert, I.M. Jazet, L.O. Martinez, L. Kritharides, J.F.P. Berbee, M.R. Boon, P. C.N. Rensen, Short-term cooling increases serum triglycerides and small high-density lipoprotein levels in humans, J. Clin. Lipidol. 11 (4) (2017) 920–928 e2.
[57] V. Ouellet, S.M. Labbe, D.P. Blondin, S. Phoenix, B. Guerin, F. Haman, E. E. Turcotte, D. Richard, A.C. Carpentier, Brown adipose tissue oxidative metabolism contributes to energy expenditure during acute cold exposure in humans, J. Clin. Invest. 122 (2) (2012) 545–552.
[58] D.P. Blondin, S.M. Labbe, C. Noll, M. Kunach, S. Phoenix, B. Guerin, E.E. Turcotte, F. Haman, D. Richard, A.C. Carpentier, Selective impairment of glucose but not fatty acid or oxidative metabolism in brown adipose tissue of subjects with type 2 diabetes, Diabetes 64 (7) (2015) 2388–2397.
[59] S.M. Gordon, H. Li, X. Zhu, A.S. Shah, L.J. Lu, W.S. Davidson, A comparison of the mouse and human lipoproteome: suitability of the mouse model for studies of human lipoproteins, J. Proteome Res. 14 (6) (2015) 2686–2695.
[60] M.C. Camus, M.J. Chapman, P. Forgez, P.M. Laplaud, Distribution and characterization of the serum lipoproteins and apoproteins in the mouse, Mus musculus, J Lipid Res 24 (9) (1983) 1210–1228.
[61] V. Guyard-Dangremont, C. Desrumaux, P. Gambert, C. Lallemant, L. Lagrost, Phospholipid and cholesteryl ester transfer activities in plasma from 14 vertebrate species, relation to atherogenesis susceptibility, Comp. Biochem. Physiol. B Biochem. Mol. Biol. 120 (3) (1998) 517–525.
[62] D.E. Chusyd, D. Wang, D.M. Huffman, T.R. Nagy, Relationships between rodent white adipose fat pads and human white adipose fat depots, Front. Nutr. 3 (2016) 10.
[63] M.A. Zuriaga, J.J. Fuster, N. Gokce, K. Walsh, Humans and mice display opposing patterns of "Browning" gene expression in visceral and subcutaneous white adipose tissue depots, Front Cardiovasc Med 4 (2017) 27.
[64] A.B. Marcher, A. Loft, R. Nielsen, T. Vihervaara, J.G. Madsen, M. Sysi-Aho, K. Ekroos, S. Mandrup, RNA-Seq and mass-spectrometry-based lipidomics reveal extensive changes of glycerolipid pathways in brown adipose tissue in response to cold, Cell Rep. 13 (9) (2015) 2000–2013.
[65] S. Virtue, A. Vidal-Puig, Adipose tissue expandability, lipotoxicity and the Metabolic Syndrome–an allostatic perspective, Biochim. Biophys. Acta 1801 (3) (2010) 338–349.
[66] D. Hauton, S.B. Richards, S. Egginton, The role of the liver in lipid metabolism during cold acclimation in non-hibernator rodents, Comp. Biochem. Physiol. B Biochem. Mol. Biol. 144 (3) (2006) 372–381.
[67] G. Pernes, P.K. Morgan, K. Huynh, N.A. Mellett, P.J. Meikle, A.J. Murphy, D. C. Henstridge, G.I. Lancaster, Characterization of the circulating and tissue-specific alterations to the lipidome in response to moderate and major cold stress in mice, Am. J. Phys. Regul. Integr. Comp. Phys. 320 (2) (2021) R95–R104.
[68] T.O. Eichmann, M. Kumari, J.T. Haas, R.V. Farese Jr., R. Zimmermann, A. Lass, R. Zechner, Studies on the substrate and stereo/regioselectivity of adipose triglyceride lipase, hormone-sensitive lipase, and diacylglycerol-O-acyltransferases, J. Biol. Chem. 287 (49) (2012) 41446–41457.
[69] R. Schreiber, C. Diwoky, G. Schoiswohl, U. Feiler, N. Wongsiriroj, M. Abdellatif, D. Kolb, J. Hoeks, E.E. Kershaw, S. Sedej, P. Schrauwen, G. Haemmerle, R. Zechner, Cold-induced thermogenesis depends on ATGL-mediated lipolysis in cardiac muscle, but not brown adipose tissue, Cell Metab. 26 (5) (2017) 753–763.e7.
[70] R. Ernst, C.S. Ejsing, B. Antonny, Homeoviscous adaptation and the regulation of membrane lipids, J. Mol. Biol. 428 (24 Pt A) (2016) 4776–4791.
[71] J. Ecker, G. Liebisch, M. Scherer, G. Schmitz, Differential effects of conjugated linoleic acid isomers on macrophage glycerophospholipid metabolism, J. Lipid Res. 51 (9) (2010) 2686–2694.
[72] H. Hauser, I. Pascher, R.H. Pearson, S. Sundell, Preferred conformation and molecular packing of phosphatidylethanolamine and phosphatidylcholine, Biochim. Biophys. Acta 650 (1) (1981) 21–51.
[73] H. Hauser, N. Gains, Spontaneous vesiculation of phospholipids: a simple and quick method of forming unilamellar vesicles, Proc. Natl. Acad. Sci. USA 79 (6) (1982) 1683–1687.
[74] U.I. Richardson, R.J. Wurtman, Polyunsaturated fatty acids stimulate phosphatidylcholine synthesis in PC12 cells, Biochim. Biophys. Acta 1771 (4) (2007) 558–563.
[75] B.A. Bladergroen, L.M. van Golde, CTP:phosphoethanolamine cytidylyltransferase, Biochim. Biophys. Acta 1348 (1–2) (1997) 91–99.
[76] A. Pawar, J. Xu, E. Jerks, D.J. Mangelsdorf, D.B. Jump, Fatty acid regulation of liver X receptors (LXR) and peroxisome proliferator-activated receptor alpha (PPARalpha ) in HEK293 cells, J. Biol. Chem. 277 (42) (2002) 39243–39250.
[77] G.S. Attard, R.H. Templer, W.S. Smith, A.N. Hunt, S. Jackowski, Modulation of CTP:phosphocholine cytidylyltransferase by membrane curvature elastic stress, Proc. Natl. Acad. Sci. USA 97 (16) (2000) 9032–9036.
[78] M.M. Manni, M.L. Tiberti, S. Pagnotta, H. Barelli, R. Gautier, B. Antonny, Acyl chain asymmetry and polyunsaturation of brain phospholipids facilitate membrane vesiculation without leakage, Elife 7 (2018).
[79] S. Ollila, M.T. Hyvonen, I. Vattulainen, Polyunsaturation in lipid membranes: dynamic properties and lateral pressure profiles, J. Phys. Chem. B 111 (12) (2007) 3139–3150.